Time domain analysis and localization of a non-local PML for dispersive wave equations

Nacéra Baara, Julien Diaz, Mounir Tlemcani

Time domain analysis and localization of a non-local PML for dispersive wave equations

Nacéra BAARA[a], Julien DIAZ[b], Mounir TLEMCANI[a,*]

[a] *Université des Sciences et Technologies d'Oran - Mohamed Boudiaf (USTOMB) Algérie*
[b] *Project-team Magique-3D, Inria, Université de Pau et des Pays de l'Adour, CNRS, France*

Abstract

In this work we design and analyze new perfectly matched layers (PML) for a dispersive waves equation : the Klein Gordon equation. We show that because of the dispersion, classical PMLs do not guarantee the convergence to zero of the error, which hampers the precision in long time simulation. We propose to consider a non-local PML for which we can obtain explicit uniform estimates for the reflected analytical solution in time domain, given by an integral representation formula. This uniform estimates ensure the convergence of the error to zero at fixed time t and guarantee the accuracy of the layer. For the implementation of the new PML, we propose a localization technique that we validate numerically.

Keywords: Klein-Gordon equation, PML, dispersion, analytical solution, Green's function, Bessel's functions, uniform error, long time stability.
2000 MSC: 35L05, 35L10, 35L20, 35A08, 35A22

1. Introduction

Evolution of gravity waves in the Navier-Stokes, Euler or shallow water equations when rotation is taken into account may propagate waves at different speeds not proportional to their wavelengths. Such a phenomena is called dispersion and is described by a parameter α in the present work. Dispersion may also be seen as the wave number in higher (three dimensions for instance) *via* a Fourier transform w.r.t. the third variable in space which leads in particular to common procedures for constructing absorbing boundary conditions for wave-like equations. We will present in this work new ideas to deal numerically with some problems of wave propagation in an unbounded dispersive medium for which we have chosen the Klein-Gordon equation as the standard model of the dispersive wave equation. The results presented in this paper are useful for authors who are interested in the dynamics of large-scale motions of the oceans and atmosphere in geophysical rotating fluid dynamics, cf. eg. [24].

*Corresponding author: mounir.tlemcani@gmail.com

Since Bérenger [8, 9], the Perfectly Matched Layer (PML) technique was introduced as an alternative for the absorbing boundary condition (ABC) method (cf. Engquist [17, 18]) to simulate the propagation of waves in unbounded domains. It consists in truncating the computational domain by an absorbing layer with a damping term acting only in the orthogonal direction for outgoing waves and having the nice property that the layer is perfectly matched at the interface. In computational codes, the most crucial drawback of PML's implementation is a stability property of the associated equations in the layer for long time simulation of the total wave field (transmitted plus reflected).

While existing results mainly concern modal or plane wave analysis for the question of stability in time domain analysis (cf. eg. [12, 1, 6]), explicit error estimates were discussed in the literature by very few authors. We refer to [16] for a detailed presentation in the case of advective acoustics in time domain with parallel mean flow. To the authors' knowledge, no such results exist for dispersive waves such as for example Klein-Gordon equation or more generally damped waves with dispersion.

Based on the Cagniard-de Hoop method [13, 10, 14, 25], known for its power in the case of stratified media, the authors in [16] have obtained analytical solution and explicit error estimates for PMLs for advective acoustics which result from the linearized Euler system. Because of the lack of homogeneity of some integrand functions in the Fourier-Laplace space, the method does not apply (at least straightforwardly) if one considers the dispersion term in designing PMLs for wave problems as in rotating shallow water [20, 2, 5], in particular for Klein-Gordon wave like equations. In our study, we propose to replace the Laplace variable, denoted by s, by a non-local one $\sqrt{s^2+\alpha^2}$ specifically including Bessel's functions when returning back to time-domain solutions [3]. Doing so, one takes into account the dispersion term denoted by α implicitly in such a way that the new forms of the equations will correspond exactly to a non-dispersive case. Thanks to this new variable, we present in this work an integral representation of the Green's function associated with the Klein Gordon equation. This expression can be derived explicitly and therefore the analytical solution follows by a convolution in time with the source term. A new non-local PML formulation is deduced and can consequently be analyzed in time-domain in a very similar way to that of [16]. We refer to [26, 12, 9, 11] (the list is not exhaustive) for more details on PMLs in time domain acoustics. Recently, the authors in [7] have shown the failure of standard PML change of variable for some dispersive cases such as the Drude model in electromagnetics. They have proposed a modification of the time frequency ω by $\omega\psi(\omega)$ where $\psi(\omega)$ is a suitable rational function of ω that ensures the stability of the absorbing layer. In our study, we present a localization technique for a particular dispersive model in acoustics (the Klein-Gordon equation) that allows us to build such functions in order to ensure both the stability and the precision of the PML for long waves adjustment. As a main result, explicit error estimates are obtained for the non-local PML's formulation associated to the Klein-Gordon equation (i.e., dispersive waves), long time stability results still hold but uniform convergence result to zero of the error failed when the time goes to infinity. In addition, a new PML based on a localization technique is proposed and shown to be better than the classical one for inertial oscillations regime that is specific to dispersive waves solutions.

In the second section, we present the main steps of constructing non-local PMLs for dispersive wave like equations in two dimensions. The third section is devoted to the computation of fundamental solution in whole (free) space (the incident Green's function) and in a half space with PML of finite width (the reflected Green's function). These fundamental solutions allow us to obtain the analytical solution of the PML's equation as a convolution (in the sense of Laplace transform) of the total field (Green's function) with the source term located in space in the physical domain. We present a fundamental lemma that permits us to write a representation formula for the fundamental solution via Bessel's functions and the Green's function of the non-dispersive wave equation. This provides a splitting of the solution as a non-dispersive part and a purely dispersive one. In the fourth section, error estimates are obtained in a very similar way to that of [16] by taking care on the behaviour for long time of an oscillating integral appearing in the dispersive part of the solution. As a result, the uniform error does not converge to zero in long time because of a term proportional to $\sqrt{\alpha}$ appearing in the upper bound, explaining therefore the fact that long time stability is conserved but the precision can be justified at most for small α. In the fifth section, a localization technique at high frequencies is presented similarly to the ABC's methodology [17] and a numerical comparison of the zeroth and first order Taylor approximations of the square root $\sqrt{\partial_t^2 + \alpha^2}$ is performed. Numerical experiments are thus presented in order to validate the effect of α on designing PMLs for dispersive waves, particularly for long waves regime which arises after very long periods in time. The last section is devoted to conclusions, comments and remarks.

2. Non-local PML for a family of 2d dispersive wave equations

Let us consider the two-dimensional family of dispersive wave equations

$$\frac{1}{c^2}\frac{\partial^2}{\partial t^2}u_\alpha - \Delta u_\alpha + \alpha^2 u_\alpha = f(x,t),\ x = (x_1, x_2) \in \mathbb{R}^2, \quad t > 0, \tag{1}$$

where $\alpha \geq 0$ is the so-called dispersion parameter. For simplicity and without restriction, we will assume in all what follows that $c = 1$. If the initial data of the problem is compactly supported in the domain of interest $\mathbb{R}^2_- = \mathbb{R}_- \times \mathbb{R}$, then it is natural to reduce computation to this left half-space. There are two main classes of methods to do so. The first ones consist in approximating the radiation condition at finite distance resulting in the so-called absorbing boundary conditions (ABC). The second ones are called perfectly matched layers (PML) and consist in adding a fictitious layer that at the same time adapts the impedance at the interface and absorbs the outgoing waves, cf. Figure 1. As this method is furthermore really easy to implement (specifically in the corners of the domain), it has rapidly attracted a lot of people in different fields of application.

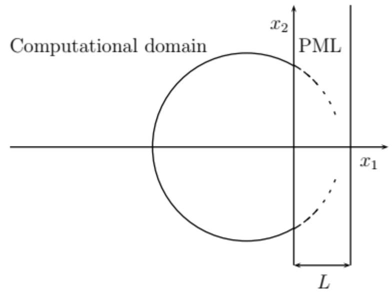

Figure 1: Computational domain and Perfectly Matched Layer

When $\alpha = 0$, and alternatively to the original idea of Bérenger (1996), PML can be implemented by adding a layer of width L in which (1) is modified via an absorption term $\sigma \geq 0$ by replacing the x_1-spatial derivative $\frac{\partial}{\partial x_1}$ in (1) by

$$D^{\sigma}_{x_1} = \left(\frac{\partial}{\partial t} + \sigma(x_1)\right)^{-1} \frac{\partial}{\partial t}\frac{\partial}{\partial x_1}. \tag{2}$$

In the present work, we propose to extend this change of variable in such a way that both perfect matching and good stability properties of the layer are conserved exactly as in the case $\alpha = 0$, i.e. without dispersion. In fact, we can achieve this at the expense of the local character of the PML as follows: the x_1-spatial derivative $\frac{\partial}{\partial x_1}$ in (1) will be replaced rather by (at least formally)

$$D^{\sigma}_{x_1,\alpha} = \left(\sqrt{\frac{\partial^2}{\partial t^2} + \alpha^2} + \sigma(x_1)\right)^{-1} \sqrt{\frac{\partial^2}{\partial t^2} + \alpha^2}\,\frac{\partial}{\partial x_1}, \tag{3}$$

in such a way that $D^{\sigma}_{x_1,0}$ coincides with the standard $D^{\sigma}_{x_1}$. The second order formulation of the PML (a vertical layer of width L) reads as follows:

$$\left(\frac{\partial^2}{\partial t^2} + \alpha^2\right) u_\alpha - \left(D^{\sigma}_{x_1,\alpha}\right)^2 u_\alpha - \frac{\partial^2}{\partial x_2^2} u_\alpha = 0,\ x = (x_1, x_2) \in (0, L)\times\mathbb{R}, t > 0. \tag{4}$$

It is well known that the homogeneous equation associated to (1) supports plane wave solutions proportional to $e^{i(\omega t - \mathbf{k}.x)}$ where ω and $\mathbf{k} = (k_1, k_2)^t$ designate the time frequency and wave vector respectively. These two parameters are related by the so-called dispersion relation $-\omega^2 + \mathrm{k}^2 + \alpha^2 = 0$ where $\mathrm{k} := \sqrt{k_1^2 + k_2^2}$ denotes the wave number. As shown in Figure 2, dispersive waves have a cut-off frequency at $\omega = \alpha$ that corresponds to inertial oscillations and appears after very long periods in time. The major difference between dispersive and non-dispersives waves can be located in the vicinity of this cut-off frequency, while for k large there is no significant distinction. It is precisely with the aim of correctly taking into account the modes close to inertial oscillations that we are led to consider the idea of non-local PMLs.

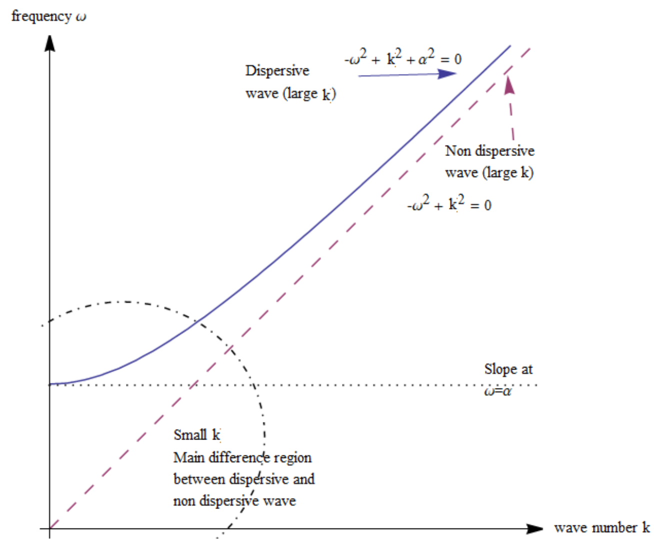

Figure 2: Dispersion relation of the KG equation in the cases $\alpha \neq 0$ (dispersive waves) and $\alpha = 0$ (non-dispersive waves).

We are thus interested in the following transmission problem with a regular point source $f(t)$ compactly supported in $[0,T)$ and located in space at $x_S = (-h,0) \in \mathbb{R}_-^* \times \mathbb{R}$ and an absorption profile $\sigma \equiv \sigma(x) > 0$ if $0 < x < L$ (L may be finite or not) and $\sigma \equiv 0$ if $x \leq 0$,

$$\begin{cases} \text{Find } u_\alpha^{\sigma,L} : (-\infty, L) \times \mathbb{R} \times \mathbb{R}_+ \to \mathbb{R}, \text{ zero for } t < 0, \\ \left(\dfrac{\partial^2}{\partial t^2} + \alpha^2\right) u_\alpha^{\sigma,L} - \left(D_{x_1,\alpha}^\sigma\right)^2 u_\alpha^{\sigma,L} - \dfrac{\partial^2 u_\alpha^{\sigma,L}}{\partial x_2^2} = \delta\left(x - x_S\right) f(t), \\ u_\alpha^{\sigma,L}\big|_{x_1 \to 0^-} = u_\alpha^{\sigma,L}\big|_{x_1 \to 0^+}, \\ \left.\dfrac{\partial u_\alpha^{\sigma,L}}{\partial x_1}\right|_{x_1 \to 0^-} = D_{x_1,\alpha}^\sigma u_\alpha^{\sigma,L}\big|_{x_1 \to 0^+}, \\ \left.\dfrac{\partial u_\alpha^{\sigma,L}}{\partial x_1}\right|_{x_1 = L} = 0, \qquad \text{if } L < +\infty. \end{cases} \tag{5}$$

Of course, the solution is assumed to be a causal and tempered distribution with support in $(-\infty, L) \times \mathbb{R} \times \mathbb{R}^+$. In the third and fourth lines of (5) we recognize the perfect matching conditions at the interface $x_1 = 0$ and in the last equation we chose a Neumann-type condition at the outer boundary $x_1 = L$. Notice that one can choose a condition of Dirichlet-type instead of Neumann with a slight change in the principle of the image to determine the analytical solution in the cas of a finite layer.

3. Integral representation of the Green's function

Following results that are presented in [16] in the case of a dispersionless media (i.e. $\alpha = 0$) with full details based on the Cagniard de-Hoop method for obtaining analytical solutions, one can deduce fundamental (Green's function) and analytical solutions associated to Problem (5). Fundamental solutions are those that correspond to $f(t) = \delta(t)$.

Let us define the two coordinate systems, $(r, \theta) \in \mathbb{R}_+ \times (0, 2\pi]$, such that $x - x_S = (r\cos\theta, r\sin\theta)^t$, which is relative to the point source $x_S = (-h, 0)$ and $(r^*, \theta^*) \in \mathbb{R}_+ \times (\pi/2, 3\pi/2]$ such that $x - x_S^* = (r^*\cos\theta^*, r^*\sin\theta^*)^t$, which is relative to the image point source $x_S^* = (h + 2L, 0)$, symmetrical to x_S w.r.t. the line $x_1 = L$, as shown in Figure 3. More precisely, one has $r^*(x) = r(x^*)$ and $\theta^*(x) = \theta(x^*)$ where x^* is the image of $x = (x_1, x_2)$ by the transformation $x^* = (2L - x_1, x_2)$. For $\sigma \equiv \sigma(x_1) > 0$ if $x_1 > 0$ and $\sigma \equiv 0$ if $x_1 \leq 0$, with the

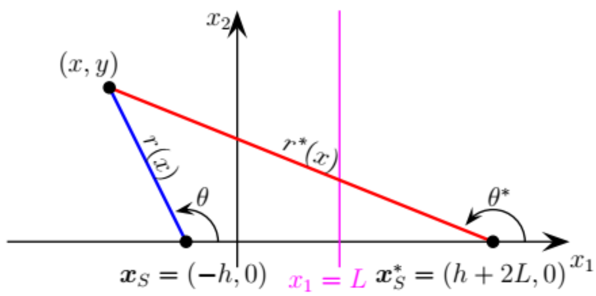

Figure 3: Coordinate system w.r.t. x_S and x_S^*.

notation $\Sigma(x_1) = \int_0^{x_1} \sigma(x)dx$, let us also define the functions

$$A(x,t) = |\cos\theta(x)|\,\Sigma(x_1)\frac{t}{r(x)}, \quad B(x,t) = |\sin\theta(x)|\,\Sigma(x_1)\sqrt{\frac{t^2}{r(x)^2} - 1}.$$

Then, we have:

- In the case of an infinite layer $(L = +\infty)$, $G_i^{\sigma,\infty}(x,t) = G_{\alpha=0,i}^{\sigma,\infty}(x,t)$ the fundamental solution of Problem (5) in a dispersionless media (i.e., for $\alpha = 0$) is given by, cf. [16, Theorem 1],

$$G_i^{\sigma,\infty}(x,t) = \frac{H\left(t - r(x)\right)}{2\pi\sqrt{t^2 - r(x)^2}} e^{-A(x,t)} \cos\left[B(x,t)\right], \quad x_1 \in \mathbb{R}.$$

- In the case of a finite layer $(L < +\infty)$, the expression of the fundamental solution $G^{\sigma,L}(x,t)$ of Problem (5) in a dispersionless media is such that

$$G^{\sigma,L}(x,t) = G_i^{\sigma,\infty}(x,t) + G_i^{\sigma,\infty}(x^*,t), \tag{6}$$

where we have extended σ symmetrically w.r.t. the line $x_1 = L$ as

$$\sigma(x_1) = \begin{cases} \sigma(x_1) & \text{if } -\infty < x_1 < L, \\ \sigma(2L - x_1) & \text{if } L < x_1 < +\infty. \end{cases}$$

The second term in the r.h.s. of (6),

$$G_i^{\sigma,\infty}(x^*, t) := G_r^{\sigma,L}(x, t)$$

is called the reflected field and admits the following expression, cf. [16, Theorem 3],

$$G_r^{\sigma,L}(x,t) = \frac{H\left(t - r(x^*)\right)}{2\pi\sqrt{t^2 - r\left(x^*\right)^2}} e^{-A(x^*,t)} \cos\left[B(x^*,t)\right], \quad x_1 \in \mathbb{R}.$$

The above results were obtained mainly in [16] with the help of the so-called Cagniard-de Hoop method which gives, handling some complex contours, a direct inversion formula for the Fourier-Laplace transform of $G_i^{\sigma,\infty}$ in the space variable x_2 and time t,

$$\tilde{\hat{G}}_i^{\sigma,\infty}(x_1, k, s) = \frac{e^{-\sqrt{k^2+s^2}\left|x_1 + h + \frac{\Sigma(x_1)}{s}\right|}}{2\sqrt{k^2 + s^2}}, \quad s > 0. \tag{7}$$

Lemma 1. *Let $\tilde{G}_\alpha(s)$ the Laplace transform of a causal function $G_\alpha(t)$, $\alpha \in \mathbb{R}_+$, such that*

$$\tilde{G}_\alpha(s) = \tilde{G}_0(\sqrt{s^2 + \alpha^2}), \tag{8}$$

then $G_\alpha(t)$ has the following integral representation

$$G_\alpha(t) = G_0(t) - \alpha \int_0^t G_0\left(\sqrt{t^2 - z^2}\right) J_1\left(\alpha z\right) dz, \tag{9}$$

where J_ν ($\nu \in \mathbb{Z}$) denotes the Bessel function of the first kind.

Proof. Direct consequence of the following inverse Laplace transform formula cf. [4, p.p. 248 – (23)],

$$\mathcal{L}^{-1}\left(e^{-hs} - e^{-h\sqrt{s^2+\alpha^2}}\right) = \frac{\alpha h J_1\left(\alpha\sqrt{t^2 - h^2}\right)}{\sqrt{t^2 - h^2}} H(t - h),$$

which yields

$$\mathcal{L}^{-1}\left(e^{-h\sqrt{s^2+\alpha^2}}\right) = \delta(t - h) - \frac{\alpha h J_1\left(\alpha\sqrt{t^2 - h^2}\right)}{\sqrt{t^2 - h^2}} H(t - h),$$

δ and H being respectively the Dirac and Heaviside functions. In fact, by causality of G_0 and linearity of $\mathcal{L}^{-1}$ applied to (8), one obtains

$$\begin{aligned}
G_\alpha(t) &= \mathcal{L}^{-1}\left(\int_0^{+\infty} G_0(t')e^{-t'\sqrt{s^2+\alpha^2}}dt'\right), \\
&= \int_0^{+\infty} G_0(t')\mathcal{L}^{-1}\left(e^{-t'\sqrt{s^2+\alpha^2}}\right)dt', \\
&= \int_0^{+\infty} G_0(t')\delta(t-t')dt' - \int_0^{+\infty} G_0(t')\frac{\alpha t' J_1\left(\alpha\sqrt{t^2-t'^2}\right)}{\sqrt{t^2-t'^2}}H(t-t')dt', \\
&= G_0(t) - \int_0^t G_0(t')\frac{\alpha t' J_1\left(\alpha\sqrt{t^2-t'^2}\right)}{\sqrt{t^2-t'^2}}dt',
\end{aligned}$$

which gives (9), using the change of variable $z = \sqrt{t^2-t'^2}$ in the last integral.
■

Theorem 1. *The expression of the fundamental solution $G_\alpha^{\sigma,L}(x,t)$ of Problem (5) for $\alpha \geq 0$ is given by*

$$G_\alpha^{\sigma,L}(x,t) = G_{\alpha,i}^{\sigma,\infty}(x,t) + G_{\alpha,r}^{\sigma,L}(x,t), \tag{10}$$

where $G_{\alpha,r}^{\sigma,L}(x,t) = 0$ if $L = +\infty$, and

$$G_{\alpha,r}^{\sigma,L}(x,t) = G_{\alpha,i}^{\sigma,\infty}(x^*,t) \qquad \text{if } L < +\infty, \tag{11}$$

$G_{\alpha,r}^{\sigma,L}(x,t)$ is the reflected field and $G_{\alpha,i}^{\sigma,\infty}(x,t)$ is the incident field and is related to the dispersionless incident field $G_i^{\sigma,\infty}(x,t)$ by the following representation formula:

$$G_{\alpha,i}^{\sigma,\infty}(x,t) = G_i^{\sigma,\infty}(x,t) - \alpha\int_0^t G_i^{\sigma,\infty}\left(x,\sqrt{t^2-z^2}\right)J_1(\alpha z)\,dz. \tag{12}$$

Proof. Let us start computing a fundamental solution for an infinite layer, i.e. $L = +\infty$. We let $f(t) = \delta(t)$ and to simplify the notation let us denote $G_\alpha^{\sigma,L}$ by G_α. Taking a Laplace-Fourier transform in time t and space x_2, $G_\alpha(.,x_2,t) \mapsto \hat{\tilde{G}}_\alpha(.,k,s)$, in the partial differential equation in Problem (5), the function $x_1 \mapsto \hat{\tilde{G}}_\alpha(x_1,k,s)$ satisfies the following ordinary differential equation with variable coefficients:

$$\left(s^2+\alpha^2+k^2\right)\hat{\tilde{G}}_\alpha - \left(\widetilde{D}_{x_1,\alpha}^\sigma\right)^2\hat{\tilde{G}}_\alpha = \delta\left(x_1+h\right), \tag{13}$$

where

$$\widetilde{D}_{x_1,\alpha}^\sigma = \left(\sqrt{s^2+\alpha^2}+\sigma(x_1)\right)^{-1}\sqrt{s^2+\alpha^2}\frac{d}{dx_1}.$$

We now use the change of variable

$$X_1(x_1,s) = x_1 + \frac{1}{\sqrt{s^2+\alpha^2}}\int_0^{x_1}\sigma(x)dx,$$

and we introduce the new unknown $\mathcal{G}_\alpha$ such that

$$\tilde{\hat{\mathcal{G}}}_\alpha\left(X_1(x_1,s),k,s\right)=\tilde{\hat{G}}_\alpha\left(x_1,k,s\right).$$

We get for $x_1>0$,

$$\frac{d\tilde{\hat{\mathcal{G}}}_\alpha}{dX_1}=\widetilde{D}^{\sigma}_{x_1,\alpha}\tilde{\hat{G}}_\alpha,$$

in such a way that the o.d.e (13) becomes

$$\left(s^2+\alpha^2+k^2\right)\tilde{\hat{\mathcal{G}}}_\alpha-\frac{d^2\tilde{\hat{\mathcal{G}}}_\alpha}{dX_1^2}=\delta\left(X_1+h\right), \tag{14}$$

which leads to the following expression of $\tilde{\hat{\mathcal{G}}}_\alpha$, for all $s>0$,

$$\tilde{\hat{\mathcal{G}}}_\alpha\left(X_1,k,s\right)=\frac{e^{-\sqrt{k^2+s^2+\alpha^2}|X_1+h|}}{2\sqrt{k^2+s^2+\alpha^2}},$$

or equivalently for $\tilde{\hat{G}}_\alpha$,

$$\tilde{\hat{G}}_\alpha\left(x_1,k,s\right)=\frac{e^{-\sqrt{k^2+s^2+\alpha^2}\left|x_1+h+\frac{\Sigma(x_1)}{\sqrt{s^2+\alpha^2}}\right|}}{2\sqrt{k^2+s^2+\alpha^2}}.$$

It is now enough to observe that

$$\tilde{\hat{G}}_\alpha\left(x_1,k,s\right)=\tilde{\hat{G}}_{0,i}\left(x_1,k,\sqrt{s^2+\alpha^2}\right). \tag{15}$$

However, $\tilde{\hat{G}}_{0,i}\left(x_1,k,s\right)$ is nothing but the Fourier-Laplace transform of $G_i^{\sigma,\infty}$ in space x_2 and time t, given in (7), which corresponds to the incident field in the dispersionless media (i.e. for $\alpha=0$). Henceforth, the relation (12) of the theorem follows by Lemma 1 and injectivity of the Fourier transform. Finaly, relations (10) and (11) follow directly by the image principle similarly as in [16] namely that the field reflected by the outer boundary of the PML is equivalent to the incident field of the image problem according to a Neumann boundary condition. The proof of the theorem is finished. ■

Remark 1. *Observe that the perfect matching property of an infinite layer at $x_1=0$ can be seen directly in the expression of the total field $G_\alpha^{\sigma,\infty}(x,t)=G_{\alpha,i}^{\sigma,\infty}(x,t)$, for all $x_1\in\mathbb{R}$, which means that no reflection holds at $x_1=0$ when the layer is infinite.*

Remark 2. *Actually, $G_{\alpha,i}^{\sigma,\infty}$ coincides on the left half-space $x_1<0$ with $G_{\alpha,i}^{0,\infty}$ which corresponds to the Green's function associated to the KG equation in the whole space $\mathbb{R}^2$ with a source located in space at x_S. Its expression is well known in the literature cf. [23], and is given by*

$$G_{\alpha,i}^{0,\infty}(x_1,x_2,t)=\frac{H(t-r(x))}{2\pi\sqrt{t^2-r(x)^2}}\cos\left(\alpha\sqrt{t^2-r(x)^2}\right). \tag{16}$$

In fact, one can also get it from the non-dispersive solution $G_{0,i}^{0,\infty}$ by applying Lemma 1.

4. Error estimates and stability result

We consider the solution $u_\alpha^{\sigma,L}$ of Problem (5) as an approximation of the solution $u_\alpha (= u_\alpha^{0,\infty})$ of the dispersive wave equation in the whole space:

$$\begin{cases} \text{Find } u_\alpha : \mathbb{R}^2 \times \mathbb{R}_+ \to \mathbb{R}, \text{ null for } t < 0, \\ \left(\dfrac{\partial^2}{\partial t^2} + \alpha^2\right) u_\alpha - \dfrac{\partial^2 u_\alpha}{\partial x_1^2} - \dfrac{\partial^2 u_\alpha}{\partial x_2^2} = \delta\left(x - x_S\right) f(t), \end{cases} \tag{17}$$

Notice that $u_\alpha^{0,\infty}$ is nothing but the restriction of $u_\alpha^{\sigma,\infty}$ to the left half-space $\mathbb{R}^2_- = \mathbb{R}_- \times \mathbb{R}$. We will give thus a time-domain analysis of the error

$$e_\alpha^{\sigma,L} = u_\alpha^{\sigma,L} - u_\alpha$$

w.r.t. to the parameters σ, L, h and α.

Remark 3. *The result (12) in Theorem 1 also applies for the total field, i.e., one has for $G_\alpha^{\sigma,L}$ the same representation formula*

$$G_\alpha^{\sigma,L}(x,t) = G^{\sigma,L}(x,t) - \alpha \int_0^t G^{\sigma,L}\left(x, \sqrt{t^2 - z^2}\right) J_1\left(\alpha z\right) dz, \tag{18}$$

which actually means that the field can be decomposed into two parts: the first one $G^{\sigma,L}(x,t)$ that is specific to a purely non-dispersive wave and the second one that is proportional to α and carries the dispersion when $\alpha \neq 0$.

We deduce that analytical solution of Problem (5) can be obtained (for a regular source term $f(t)$) by a convolution in time in the sense of Laplace transform as follows:

$$u_\alpha^{\sigma,L}\left(x,t\right) = \int_0^{+\infty} G_\alpha^{\sigma,L}\left(x,\tau\right) f\left(t - \tau\right) d\tau.$$

Following Remark 3 and using the representation formula (18), it follows that the analytical solution $u_\alpha^{\sigma,L}\left(x,t\right)$ admits also a similar representation, i.e.,

$$u_\alpha^{\sigma,L}(x,t) = u^{\sigma,L}(x,t) - \alpha \int_0^t u^{\sigma,L}\left(x, \sqrt{t^2 - z^2}\right) J_1\left(\alpha z\right) dz, \tag{19}$$

which implies also that the same happens for the error function $e_\alpha^{\sigma,L}(x,t)$, i.e.

$$e_\alpha^{\sigma,L}(x,t) = e^{\sigma,L}(x,t) - \alpha \int_0^t e^{\sigma,L}\left(x, \sqrt{t^2 - z^2}\right) J_1\left(\alpha z\right) dz. \tag{20}$$

Here, $e^{\sigma,L}(x,t)$ is the error (or reflected field) without dispersion that has been fully studied in [16, Theorem 4]. After having redefined the time function $\Phi(t)$, null for $t < 2L + h$, by:

$$\Phi(t) = \begin{cases} 0 & \text{if } t \leq 2L + h, \\ \ln\left(\dfrac{t + \sqrt{t^2 - (2L+h)^2}}{2L+h}\right) & \text{if } 2L + h < t \leq 2L + h + T, \\ \ln\left(\dfrac{t + \sqrt{t^2 - (t-T)^2}}{(t-T)}\right) & \text{if } t > 2L + h + T, \end{cases} \tag{21}$$

we recall that this error is bounded by

$$\left\| e^{\sigma,L}(.,t) \right\|_{L^\infty\left(\mathbb{R}^2_-\right)} \leq \frac{1}{2} e^{-2\Sigma(L)\frac{2L+h}{t}} \Phi(t) \left\| f \right\|_{L^\infty}, \tag{22}$$

in such a way that for $T < \infty$, $\Phi(t)$ behaves for large t as $\mathcal{O}(\sqrt{2T/t})$ and $e^{\sigma,L}(.,t)$ converges uniformly to 0 as t tends to $+\infty$, for all σ, L and h. One can show that Φ is a positive and continuous function increasing for $2L+h < t < 2L+h+T$ and decreasing for $t > 2L+h+T$, hence $\Phi(t)$ reaches its maximum at $t = 2L + h + T$, i.e.

$$\max_{t \geq 0} \Phi(t) = \Phi_{max} = \Phi\left(2L + h + T\right) \tag{23}$$

The following Lemma gives uniform bound of an oscillating integral useful for the error estimate in the dispersive case, i.e. when α is non zero.

Lemma 2. *Let $\Phi(t)$ given by (21), then*

$$\alpha \int_0^t \Phi\left(\sqrt{t^2 - z^2}\right) \left| J_1\left(\alpha z\right) \right| dz \leq M(t) \sqrt{2\alpha},$$

where

$$M(t) = \begin{cases} 0 & \textit{if } t \leq 2L + h, \\ T_0 \Phi_{max} & \textit{if } 2L + h < t \leq 2L + h + 2T, \\ T_0 \Phi_{max} + 12\sqrt{T}\left(1 + 2\sqrt{\dfrac{T}{t}}\right) & \textit{if } t > 2L + h + 2T, \end{cases}$$

Φ_{max} is given by (23) and $T_0 > 0$ is defined by

$$T_0 = 2\left(\left(2L + h + 2T\right)^2 - \left(2L + h\right)^2\right)^{\frac{1}{4}}.$$

Proof. With the help of the change of variable $z = \sqrt{t^2 - x^2}$,

$$\alpha \int_0^t \Phi\left(\sqrt{t^2 - z^2}\right) \left| J_1\left(\alpha z\right) \right| dz = \alpha \int_0^t \Phi\left(x\right) \frac{x}{\sqrt{t^2 - x^2}} \left| J_1\left(\alpha \sqrt{t^2 - x^2}\right) \right| dx,$$

and by the following Bessel's function property, cf. [22]: the fact that for $\alpha > 0$ and for all $z > 0$,

$$|J_1(\alpha z)| \leq \sqrt{\frac{2}{\alpha z}}, \tag{24}$$

one obtains the inequality

$$\alpha \int_0^t \Phi(x) \frac{x}{\sqrt{t^2 - x^2}} \left| J_1\left(\alpha\sqrt{t^2 - x^2}\right) \right| dx \leq \sqrt{2\alpha} \int_0^t \Phi(x) \frac{x}{(t^2 - x^2)^{\frac{3}{4}}} dx. \tag{25}$$

Henceforth, if $t \leq 2L + h$ then by definition $\Phi(x) = 0$ for all $x \in (0, t)$ and the r.h.s. of (25) is zero. Moreover, if $2L + h < t \leq 2L + h + 2T$ then one has

$$\begin{aligned} r.h.s.(25) &= \sqrt{2\alpha} \int_{2L+h}^t \Phi(x) \frac{x}{(t^2 - x^2)^{\frac{3}{4}}} dx, \\ &\leq \sqrt{2\alpha} \max_x \Phi(x) \int_{2L+h}^{2L+h+2T} \frac{x}{(t^2 - x^2)^{\frac{3}{4}}} dx = \sqrt{2\alpha}\Phi_{max} T_0. \end{aligned}$$

Furthermore, if $t > 2L + h + 2T$ then with the help of the standard inequality : $\log Z \leq Z - 1$ which holds for all $Z \geq 1$, one can write

$$\begin{aligned} \Phi(x) = \ln\left(\frac{x + \sqrt{x^2 - (x-T)^2}}{(x-T)}\right) &\leq \frac{T + \sqrt{T(2x - T)}}{x - T} \\ &\leq \frac{T + \sqrt{T(2x - 2T + T)}}{x - T} \\ &\leq \frac{2T}{x - T} + \sqrt{\frac{2T}{x - T}}. \end{aligned}$$

Hence, if $x > 2L+h+2T$ then $x > 2T$ which yields $x-T > x/2$ and consequently the following estimate holds:

$$\Phi(x) \leq \frac{4T}{x} + \sqrt{\frac{4T}{x}}, \ \forall x \in (2L + h + 2T, t).$$

One concludes that

$$\int_{2L+h+2T}^t \Phi(x) \frac{x}{(t^2 - x^2)^{\frac{3}{4}}} dx \leq \int_0^t \frac{4T + 2\sqrt{Tx}}{(t^2 - x^2)^{\frac{3}{4}}} dx. \tag{26}$$

On the other hand, using a change of variable $x = t\sqrt{z}$, one has using the definition of the Euler integral of the first kind

$$\beta(u, v) = \int_0^1 z^{u-1} (1 - z)^{v-1} dz,$$

which is defined for $\Re e(u) > 0$ and $\Re e(v) > 0$,

$$\int_0^t x^\lambda \left(t^2 - x^2\right)^\mu dx = t^{\lambda+2\mu+1} \int_0^1 z^{\frac{\lambda-1}{2}} (1-z)^\mu dz$$
$$= t^{\lambda+2\mu+1} \beta\left(\frac{\lambda+1}{2}, \mu+1\right),$$

which in turn exists for $\Re e(\lambda) > -1$ and $\Re e(\mu) > -1$. Henceforth, the r.h.s. of (26) can be calculated, with the help of the previous identity, as follows:

$$\begin{aligned}\int_0^t \frac{4T + 2\sqrt{Tx}}{(t^2 - x^2)^{\frac{3}{4}}} dx &= \int_0^t \frac{4T}{(t^2 - x^2)^{\frac{3}{4}}} dx + \int_0^t \frac{2\sqrt{Tx}}{(t^2 - x^2)^{\frac{3}{4}}} dx,\\ &= 4T \int_0^t x^0 \left(t^2 - x^2\right)^{-\frac{3}{4}} dx + 2\sqrt{T} \int_0^t x^{\frac{1}{2}} \left(t^2 - x^2\right)^{-\frac{3}{4}} dx,\\ &= 4Tt^{-\frac{1}{2}} \beta\left(\frac{1}{2}, \frac{1}{4}\right) + 2\sqrt{T} t^0 \beta\left(\frac{3}{4}, \frac{1}{4}\right),\\ &\leq 12\sqrt{T}\left(2\sqrt{\frac{T}{t}} + 1\right),\end{aligned}$$

since one has

$$\beta\left(\frac{3}{4}, \frac{1}{4}\right) < \beta\left(\frac{1}{2}, \frac{1}{4}\right) < 6.$$

Thus, if $t > 2L + h + 2T$ then by the decomposition

$$\int_0^t = \int_0^{2L+h} + \int_{2L+h}^{2L+h+2T} + \int_{2L+h+2T}^t,$$

one concludes that

$$\alpha \int_0^t \Phi\left(\sqrt{t^2 - z^2}\right) |J_1(\alpha z)| \, dz \leq \left(T_0 \Phi_{max} + 12\sqrt{T}\left(1 + 2\sqrt{\frac{T}{t}}\right)\right)\sqrt{2\alpha}, \tag{27}$$

which ends the proof of the Lemma. ■

Theorem 2. *For a regular source term $f(t)$ compactly supported in $[0, T)$, $T < +\infty$, the error $e_\alpha^{\sigma,L}(.,t) = u_\alpha^{\sigma,L}(.,t) - u_\alpha(.,t)$ is null for $t < 2L + h$, and for all $t \geq 2L + h$ the following estimate holds:*

$$\left\|e_\alpha^{\sigma,L}(.,t)\right\|_{L^\infty(\mathbb{R}^2_-)} \leq \frac{1}{2} e^{-2\Sigma(L)\frac{2L+h}{t}} \|f\|_{L^\infty} \left(\Phi(t) + M(t)\sqrt{2\alpha}\right), \tag{28}$$

where $M(t)$ is defined in Lemma 2.

Proof. Thanks to Inequality (22) it will be enough to estimate the second term in the r.h.s. in the representation formula (20). So, one has again by Inequality (22):

$$\begin{aligned}\left\| e_{\alpha}^{\sigma,L}(.,t) - e^{\sigma,L}(.,t) \right\|_{L^{\infty}\left(\mathbb{R}^2_-\right)} &= \sup_{x\in\mathbb{R}^2_-} \left| \alpha \int_0^t e^{\sigma,L}\left(x, \sqrt{t^2-z^2}\right) J_1(\alpha z)\, dz \right| \\ &\leq \frac{\alpha}{2} \|f\|_{L^{\infty}} \int_0^t e^{-2\Sigma(L)\frac{2L+h}{\sqrt{t^2-z^2}}} \Phi\left(\sqrt{t^2-z^2}\right) |J_1(\alpha z)|\, dz.\end{aligned} \tag{29}$$

With the help of the triangular inequality, one has

$$\left\| e_{\alpha}^{\sigma,L}(.,t) \right\|_{L^{\infty}\left(\mathbb{R}^2_-\right)} \leq \left\| e_{\alpha}^{\sigma,L}(.,t) - e^{\sigma,L}(.,t) \right\|_{L^{\infty}\left(\mathbb{R}^2_-\right)} + \left\| e^{\sigma,L}(.,t) \right\|_{L^{\infty}\left(\mathbb{R}^2_-\right)}.$$

Moreover,

$$\sup_{z\in(0,t)} e^{-2\Sigma(L)\frac{2L+h}{\sqrt{t^2-z^2}}} = e^{-2\Sigma(L)\frac{2L+h}{t}},$$

then (22) implies that the r.h.s of (29) is bounded from above by

$$\frac{\alpha e^{-2\Sigma(L)\frac{2L+h}{t}} \|f\|_{L^{\infty}}}{2} \int_0^t \Phi\left(\sqrt{t^2-z^2}\right) |J_1(\alpha z)|\, dz. \tag{30}$$

Henceforth, the proof of the theorem follows by Lemma 2 and Inequality (22). In particular, the error is zero for $t < 2L+h$ since $\Phi(t) = M(t) = 0$ for all $t < 2L+h$. ■

It should be pointed that the presence of the function $M(t)$ in the r.h.s. of the estimate (28) can be interpreted as a result of stability only. More precisely, we can see that for t large, $M(t)$ does not have the same asymptotic behavior as $\Phi(t)$. Indeed, $M(t) = \sqrt{\alpha}\mathcal{O}(1)$ while $\Phi(t) = \mathcal{O}\left(t^{-1/2}\right)$.

5. Localization and numerical application

The operator $D^{\sigma}_{x_1,\alpha}$ that appears in the PML change of variable (3) is non-local. Therefore, we propose a localization technique at high frequencies similarly to the ABC's methodology [17]. As an example, comparisons (numerical and plane waves analysis) of the zeroth and first order Taylor approximations of the square root $\sqrt{\partial_t^2 + \alpha^2}$ are feasible and will be sufficient to put in evidence the effect of the dispersion parameter α.

5.1. Localization

The expression of the PML equation obtained in Section 2 is non-local since a square root appears in the change of variable (3), which is far from being practical in a numerical application. A standard zeroth-order approximation at high frequencies can be used, just as usually done by the authors when dealing with dispersive wave equation by taking (for example) simply $\alpha = 0$ in (3) to obtain the standard form of $D^{\sigma}_{x_1}$ as given by (2), (cf. eg. [2, 5, 27]). Instead of that, we propose here a new family of PML's operators by a localization technique that can be based on a Taylor or any other asymptotic expansion (such as Padé's approximation) of the square root $\sqrt{s^2+\alpha^2}$ at high frequencies (of a specific order). It is similar to those used in designing absorbing boundary conditions ([17, 18, 20, 15, 27]). At high frequencies $\alpha \ll s$, one can write

$$\sqrt{s^2+\alpha^2} = s + \frac{1}{2}\alpha^2 s^{-1} + \mathcal{O}\left(\frac{\alpha}{s}\right)^4. \tag{31}$$

The computation of $\xi = D^{\sigma}_{x_1,\alpha}\phi$ can be done by inverting the operator corresponding to the symbol $\sqrt{s^2+\alpha^2}+\sigma$ in the equation, i.e.,

$$\left(\sqrt{s^2+\alpha^2}+\sigma\right)\xi = \sqrt{s^2+\alpha^2}\,\frac{d}{dx_1}\phi, \tag{32}$$

and at high frequencies $\alpha \ll s$, the square root $\sqrt{s^2+\alpha^2}$ may be replaced by dropping the highest order terms in the expansion (31) in such a way that (32) can be approximated by the equation

$$\left(s+\frac{1}{2}\alpha^2 s^{-1}+\sigma\right)\xi = \left(s+\frac{1}{2}\alpha^2 s^{-1}\right)\frac{d}{dx_1}\phi,$$

and, which up to a multiplication by s, gives

$$\left(s^2+\frac{1}{2}\alpha^2+\sigma s\right)\xi = \left(s^2+\frac{1}{2}\alpha^2\right)\frac{d}{dx_1}\phi.$$

Hence, the localization of $D^{\sigma}_{x_1,\alpha}$ (by a Taylor approximation) can be done by solving a Cauchy problem as follows:

$$\begin{cases} \left(\dfrac{\partial^2}{\partial t^2}+\dfrac{1}{2}\alpha^2+\sigma\dfrac{\partial}{\partial t}\right)\xi\,(x,t) = \left(\dfrac{\partial^2}{\partial t^2}+\dfrac{1}{2}\alpha^2\right)\dfrac{\partial}{\partial x_1}\phi\,(x,t)\,, \quad x_1>0, \\ \dfrac{\partial}{\partial t}\xi\,(x,t)\Big|_{t=0} = 0, \end{cases} \tag{33}$$

together with the perfect matching condition

$$\xi\,(x,t)|_{x_1=0^+} = \frac{\partial}{\partial x_1}\phi\,(x,t)\Big|_{x_1=0^-}$$

and the fact that the auxiliary variable ξ lives only in the PML layer $x_1>0$, i.e.,

$$\xi\,(x,t) = 0,\ x_1<0.$$

We will call the Taylor approximation given by the PML equation in the form (33) the $\alpha-$PML in the numerical results thereafter. Notice that in the case of infinite layers, both the standard PML and $\alpha-$ PML are by construction perfectly matched at the interface $x_1 = 0$. In fact, to each one corresponds the following complex change of variable:

$$X_1(x_1, s) = x_1 + \frac{1}{s}\int_0^{x_1} \sigma(x)dx, \tag{34}$$

for the standard, and

$$X_1(x_1, s) = x_1 + \frac{1}{s + \frac{1}{2}\alpha^2 s^{-1}}\int_0^{x_1} \sigma(x)dx,$$

for the $\alpha-$PML. Note also that when a finite layer of width L is used one has to add for example a homogeneous Neumann boundary condition on ξ in order to close the equations. Let us point out that a standard PML formulation will correspond to a zeroth order approximation in (32), i.e., by taking $\alpha = 0$ in (33).

5.2. Plane waves analysis

The homogeneous non-dispersive wave equation ($\alpha = 0$) admits outgoing plane wave solutions in the direction of increasing x_1 of the following form

$$U = e^{i\omega t - ik_1 x_1 + ik_2 x_2}, \quad \frac{k_1}{\omega} > 0, \tag{35}$$

where the time and space frequencies are related by the dispersion relation $\omega^2 - k_1^2 - k_2^2 = 0$.

It is well known that, when considering a finite layer(corresponding th the standard PML change of variable (34) with $s = i\omega$) of width L with homogeneous Neumann boundary condition at $x_1 = L$, then the image principle allows one to obtain through simple reflection a plane wave solution of the form

$$\begin{aligned}
u(X,t) &= U(X,t) + U(X^*,t),\\
&= e^{i(\omega t - k_1 X_1 + k_2 x_2)} + e^{i(\omega t - k_1(2L - X_1) + k_2 x_2)},\\
&= e^{i(\omega t - k_1 X_1 + k_2 x_2)} + e^{i(\omega t - k_1(2L - X_1) + k_2 x_2)},\\
&= e^{i(\omega t - k_1 x_1 + k_2 x_2)} e^{-\frac{k_1}{\omega}\int_0^{x_1}\sigma(\xi)d\xi} + e^{i(\omega t - k_1(2L - x_1) + k_2 x_2)} e^{-\frac{k_1}{\omega}\int_0^{2L - x_1}\sigma(\xi)d\xi},
\end{aligned}$$

so that in the region $x < 0$ the solution becomes

$$u(x,t) = e^{i(\omega t - k_1 x_1 + k_2 x_2)} + R_\sigma e^{i(\omega t + k_1 x_1 + k_2 x_2)},$$

where

$$R_\sigma = e^{-\frac{k_1}{\omega}\int_0^{2L - x_1}\sigma(\xi)d\xi} e^{-2ik_1 L}.$$

Moreover, one has for $x_1 < 0$,

$$\int_0^{2L - x_1} \sigma(\xi)d\xi = 2\int_0^L \sigma(\xi)d\xi$$

since σ was extended symmetrically w.r.t. the line $x_1 = L$. We thus find the reflection coefficient at the interface $x_1 = 0$:

$$R_\sigma = e^{-2\frac{k_1}{\omega}\int_0^L \sigma(\xi)d\xi} \times e^{-2ik_1L}, \tag{36}$$

where the first term in the r.h.s. of (36) is associated with absorption and the second represents a phase shift.

Similarly to the change of Laplace variable s by $\sqrt{s^2+\alpha^2}$ that we used in Section 3, we propose to analyze the reflectivity of the non-local PML for the KG equation as follows. The frequency change of variable ω by $\sqrt{\omega^2-\alpha^2}$ in (35) transforms the plane wave solution of the non-dispersive wave equation to a plane wave solution of the KG equation of the form

$$U_\alpha = e^{i\sqrt{\omega^2-\alpha^2}t - ik_1x_1 + ik_2x_2},$$

in such a way that the expression of the reflection coefficient of the finite width non-local PML at the interface $x_1 = 0$ writes as

$$R_{\sigma,\alpha} = e^{-2\frac{k_1}{\sqrt{\omega^2-\alpha^2}}\int_0^L \sigma(\xi)d\xi} \times e^{-2ik_1L}. \tag{37}$$

Henceforth, a Taylor series of the square root $\sqrt{\omega^2-\alpha^2}$ at high frequencies ($\alpha \ll \omega$) will give the following approximations of $R_{\sigma,\alpha}$, at increasing orders:

$$R^{(0)}_{\sigma,\alpha} = e^{-2\frac{k_1}{\omega}\int_0^L \sigma(\xi)d\xi} \times e^{-2ik_1L},$$

$$R^{(1)}_{\sigma,\alpha} = e^{-2\frac{k_1}{\omega-\frac{\alpha^2}{2\omega}}\int_0^L \sigma(\xi)d\xi} \times e^{-2ik_1L}, \ldots$$

These coefficients correspond exactly and respectively to the coefficients of reflection at $x_1 = 0$ of the standard ($0-$PML) and the $\alpha-$PML,..., associated with the KG equation. As a result, we have for all $\alpha > 0$ and k_1, ω such that $\omega \geq \alpha$ and $k_1/\omega > 0$,

$$\left|R^{(1)}_{\sigma,\alpha}\right| < \left|R^{(0)}_{\sigma,\alpha}\right|,$$

which means that the $\alpha-$PML improves the standard PML. Better yet, the improvement is optimal at long waves which have frequencies close to α. Indeed, one has the ratio

$$\left|\frac{R^{(1)}_{\sigma,\alpha}}{R^{(0)}_{\sigma,\alpha}}\right| = e^{-2\frac{k_1}{\omega}\frac{\alpha^2}{2\omega^2-\alpha^2}\int_0^L \sigma(\xi)d\xi} \tag{38}$$

that is increasing w.r.t. $\omega \in [\alpha, +\infty[$ and henceforth is minimal at $\omega = \alpha$. We conclude this by remarking that, at least for plane waves, $\alpha-$PML performs better than the standard one and better still for long waves, i.e., in the vicinity of the cut-off frequency α. Otherwise, the two methods (standard and $\alpha-$PMLs) are virtually identical for short waves (high frequencies $\omega \gg \alpha$) or in general for weakly dispersive waves ($\alpha \simeq 0$).

Remark 4. *The localization process in this section is based on the high frequency/short wave ($s >> \alpha$) assumption, and yet the new formulation is aimed to deal with the long waves (s close to α). In fact, the localization is expected to be less accurate for the more dispersive waves if one uses only few terms in the Taylor expansion. Other asymptotic expansion such as Padé's approximation of the square root $\sqrt{s^2+\alpha^2}$ at high frequencies may actually performs better with a slightly higher cost resulting from the quasi-localization by rational fractions.*

Remark 5. *Currently there is no reason to believe in the long-time stability of either 0-PML or $\alpha-$ PML in terms of analytical solutions. Nevertheless, a plane wave analysis with an infinite layer based on the slowness curves can be carried out without difficulty in order to show their stability at least for exponential modes as in [5, 6, 7].*

5.3. Numerical examples

In what follows, we will present results for both the standard ($0-$PML) and the $\alpha-$PML in order to discuss the effect of taking or not α into account for the precision of computations. The numerical solutions are obtained by a finite difference time-domain code (FDTD) based on a standard central finite difference scheme of leap-frog type, second order accurate in space and time, where the source function is a truncated first derivative of a Gaussian :

$$f(t) = \frac{d}{dt}\left\{e^{-2\pi f_0 (t-t_0)^2}\right\} H(2t_0 - t), \qquad f_0 = 10, \qquad t_0 = \frac{1}{f_0}.$$

It produces for $c = 1$ a wavelength $\lambda = c/f_0 = 0.1$. The space step size Δx is chosen equal in both direction x_1 and x_2, such that $\Delta x = \lambda/16$, i.e., 16 points per wavelength, with a CFL condition such that $c\Delta t/\Delta x = 0.5$.

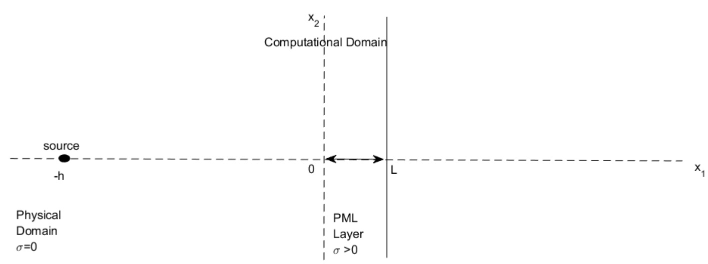

Figure 4: Configuration of the computational and physical domains and the vertical layer of width L. The source lies in the physical media outside the interface.

Let us point out that a layer in the x_2 direction (the horizontal layer) can be constructed straightforwardly by symmetry from the x_1 direction (the vertical layer). The corner layers are constructed side by side of the vertical and horizontal ones without any special care as is commonly used in PML techniques for the wave equation. We used natural transmission conditions and the numerical results show no reflection at the interfaces separating the two layers. In order to perform a long time simulation, we consider a rectangular physical domain $[-60\Delta x, 0] \times [-30\Delta x, 30\Delta x]$ completely surrounded by vertical and horizontal layers of same width $L = 20\Delta x$ and the point source is assumed located at $X_S = (-30\Delta x, 0)$. Our interest is focused only on the behaviour of the right vertical layer $0 < x_1 < L$ (cf. Figure 4) since it will be adequate to conclude later. The damping function $\sigma(x_1) = \sigma_{max} x_1^2/L$ is chosen quadratic with an empirical maximum value $\sigma_{max} = 48$. An observation point x_R (the receiver) at normal incidence is chosen on the x_1-axis at left two-points away from the interface between physical domain and PML layer.

- *Comparison of FDTD and convolution analytical solutions*

Dispersion appears at very long periods in time, which results in an adjustment of long waves towards the inertial oscillations of frequencies α. We have thus computed the analytical solution $u_\alpha(x_R, t)$ via the Maple software by calculating oscillating convolution integrals involving a cosine function (cf. Eq.(16)) to match with the finite difference reference solution. Figures 5 and 6 show the long waves adjustment of the analytical solution computed by the software Maple with $\alpha = 0.1 f_0$ (weak dispersion) and with $\alpha = 0.9 f_0$ (strong dispersion) respectively. We have also computed the analytical (or reference) solution by the finite difference code on a much larger computational domain $[-500\Delta x, 0] \times [-250\Delta x, 250\Delta x]$ by setting $\sigma = 0$ and where the simulation time $T_R = 900\Delta t$ is chosen so that the reflected wave will not have reached the outer boundary yet. Figures 7 and 8 show comparisons for short waves adjustment of the analytical solution computed by the software Maple and the FDTD code, where we have set $\alpha = 0.1 f_0$ for weak dispersion and $\alpha = 0.9 f_0$ for strong dispersion respectively. The two solutions (convolution and FDTD) are in good agreement in each case. Figures 9 and 10 show relative error incurred by the FDTD code w.r.t. the convolution integral formula to obtain analytical solution respectively for weak dispersion ($\alpha = 0.1 f_0$) and strong dispersion ($\alpha = 0.9 f_0$).

From now on, and since very long time simulation is needed later for long waves, we will use the convolution solution as the reference analytical solution for the error analysis of both the standard and $\alpha-$PML.

- *Short waves analysis of PMLs*

We will first make a comparison between the standard PML and the $\alpha-$PML during the passage of the short wave, say for $t \in [0, 900\Delta t]$, by computing the relative error produced by each method w.r.t. the analytical solution. Denoting by $u_\alpha(x_R, t)$ the PML (standard or $\alpha-$) solution, the relative error is defined by

$$E_\alpha^{\sigma, L}(x_R, t) = \frac{|u_\alpha(x_R, t) - u_{ref}(x_R, t)|}{\max_{0 \le t \le 900\Delta t} |u_{ref}(x_R, t)|}$$

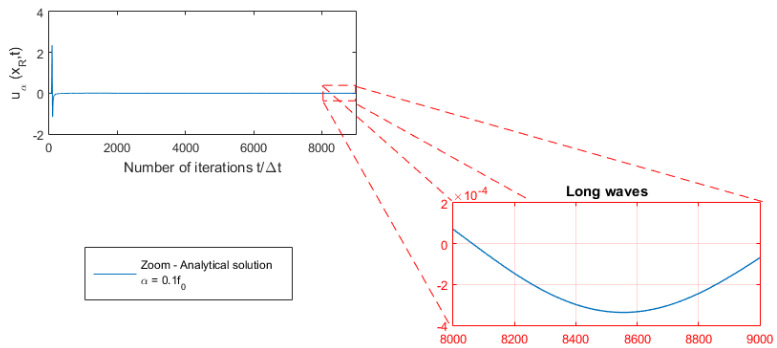

Figure 5: Weak dispersion: Zoom close to inertial oscillations adjustment of the analytical solution computed by Maple with $\alpha = 0.1f_0$.

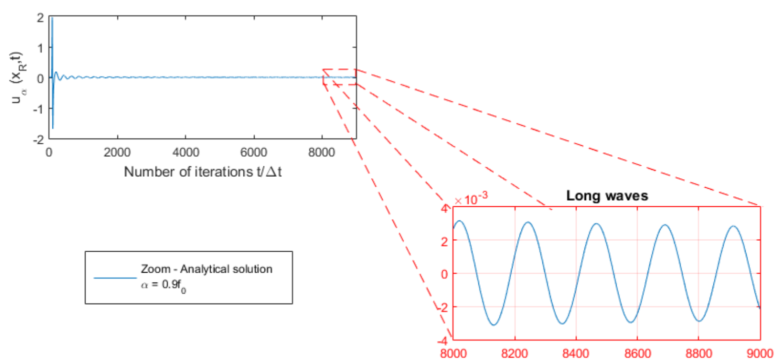

Figure 6: Strong dispersion: Zoom close to inertial oscillations adjustment of the analytical solution computed by Maple with $\alpha = 0.9f_0$.

and it is calculated for $\alpha = 0.1f_0$ (weak dispersion) and $\alpha = 0.9f_0$ (strong dispersion) respectively. In the two cases we have tested the standard PML and the $\alpha-$PML. Results for short waves are shown in Figures 11 and 12 respectively. According to the tolerance obtained in Figures 9 and 10 between the Convolution and FDTD analytical solutions, both standard PML and $\alpha-$PML performs with the same precision. One can conclude that, at least for short waves, one can continue using the standard PML without having recourse to the second method ($\alpha-$PML), as it is done in the literature for dispersive problems (cf. eg. [2, 5, 27]).

- *Long waves analysis of PMLs*

In order to highlight the positive contribution of $\alpha-$PML w.r.t. the standard, we will focus on the long time periods (for example $t \geq 900\Delta t$) during which long waves adjustment occurs (in particular the case of a strong dispersion

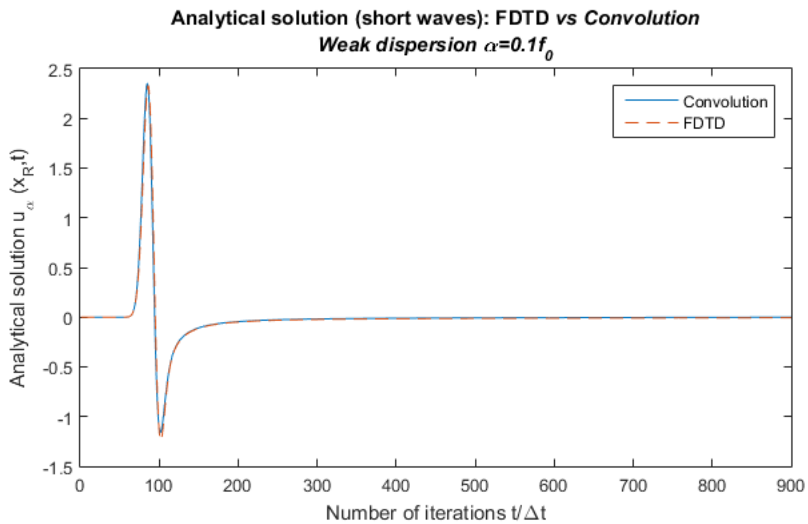

Figure 7: Weak dispersion $\alpha = 0.1f_0$: Convolution *vs* FDTD

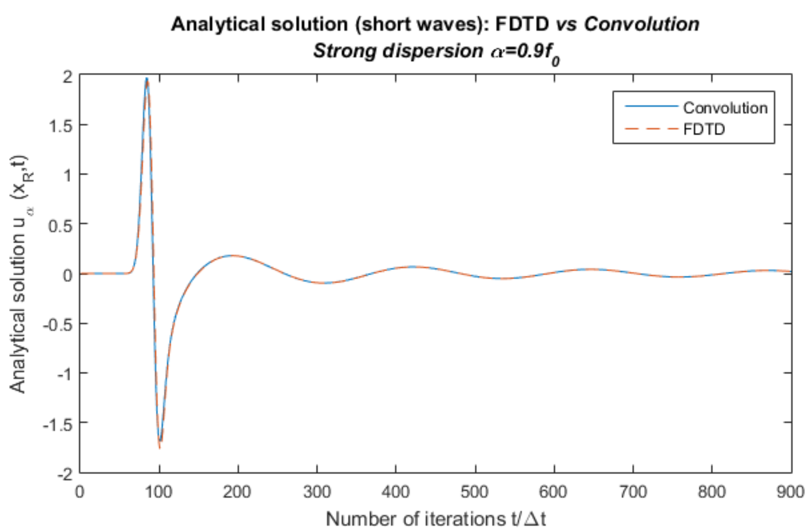

Figure 8: Strong dispersion $\alpha = 0.9f_0$: Convolution *vs* FDTD

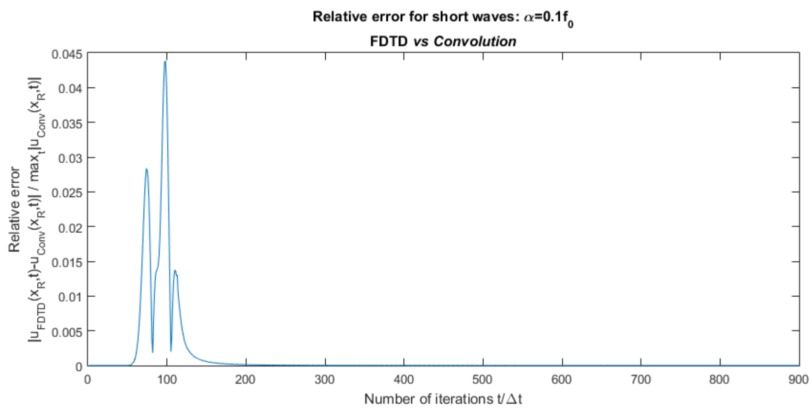

Figure 9: Relative error for short waves for $\alpha = 0.1 f_0$: FDTD *vs* Convolution solution.

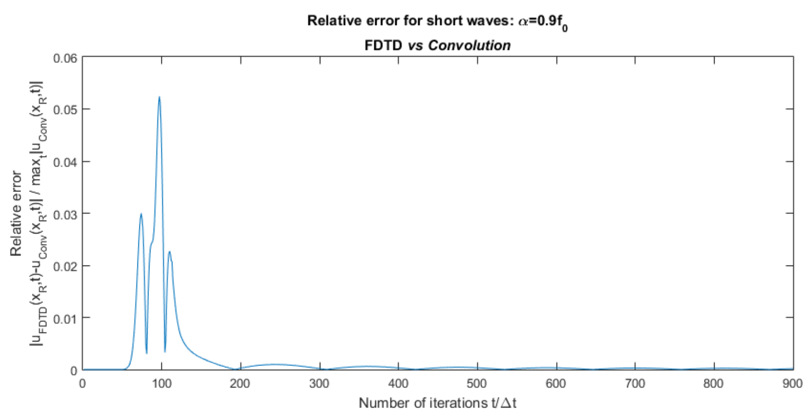

Figure 10: Relative error for short waves for $\alpha = 0.9 f_0$: FDTD *vs* Convolution solution.

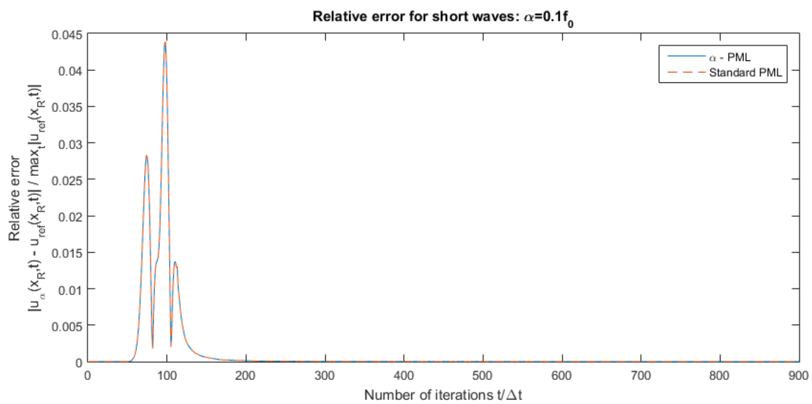

Figure 11: Weak dispersion, $\alpha = 0.1 f_0$: relative error of standard PML and $\alpha-$PML w.r.t. analytical solution.

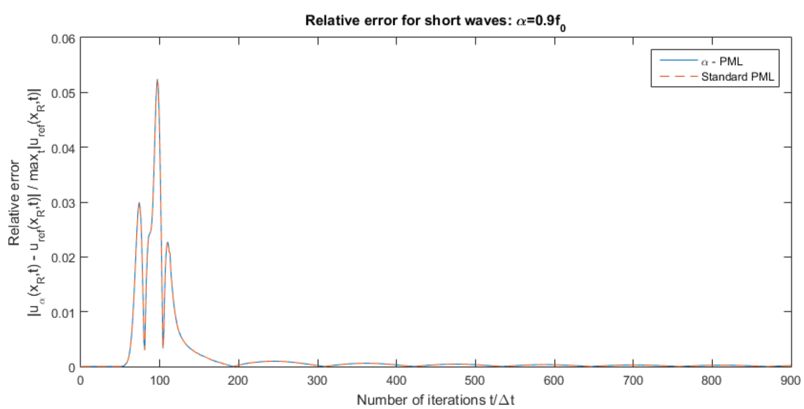

Figure 12: Strong dispersion, $\alpha = 0.9 f_0$: relative error of standard PML and $\alpha-$PML w.r.t. analytical solution.

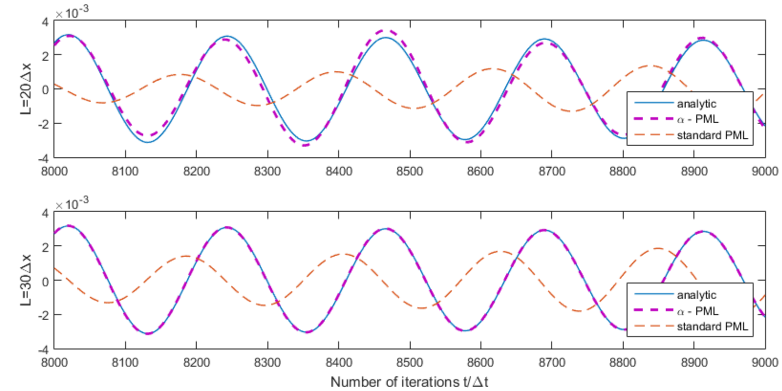

Figure 13: Comparison of standard and $\alpha-$ PMLs for long waves.

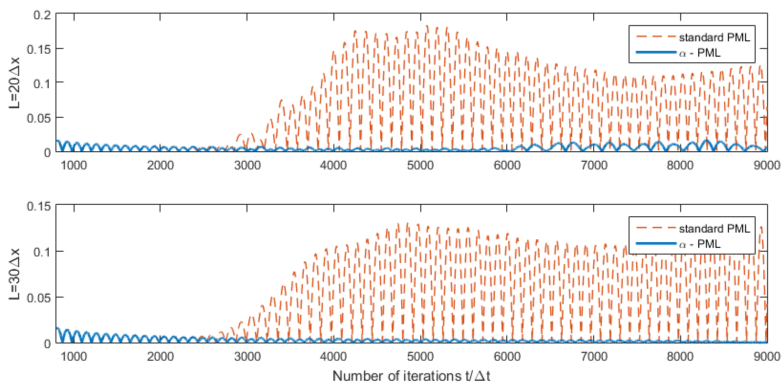

Figure 14: Relative error of standard and $\alpha-$PMLs for long waves.

$\alpha = 0.9f_0$). The relative error produced by each method w.r.t. the analytical solution is defined now by

$$E_{\alpha}^{\sigma,L}\left(x_R,t\right) = \frac{\left|u_{\alpha}\left(x_R,t\right) - u_{ref}\left(x_R,t\right)\right|}{\max_{900\Delta t \le t \le 9000\Delta t}\left|u_{ref}\left(x_R,t\right)\right|},$$

where $u_{\alpha}(x_R,t)$ denotes now the PML (standard or $\alpha-$) solution. We have tested two cases of the width of the PML layer, $L = 20\Delta x$ and $L = 30\Delta x$ for each method respectively. Figure 14 shows, for a last sample of time interval $t \geq 800\Delta t$, a comparison of long waves adjustment obtained by the standard and $\alpha-$PML *vs* the analytical solution, top picture with $L = 20\Delta x$ and bottom with $L = 30\Delta x$. We observe remarkably good agreement of the $\alpha-$PML solution with the analytical one while the one given by the standard PML remains visibly far from this adjustment. Even more precisely, in Figure 14 we observe that the relative error incurred by the $\alpha-$PML is much less significant than that produced by the standard for $L = 20\Delta x$ at top picture. Better yet at bottom, it is even decreasing in time for $L = 30\Delta x$, whereas that produced by the standard remains just bounded and above all relatively significant by comparison with the $\alpha-$PML. This is also in good agreement with the behaviour for ω close to α of the ratio of reflection coefficients given by (38) in the plane wave analysis above.

6. Conclusion

- As a principal consequence of Theorem 2, the error is not affected by the dispersion term α at a fixed time $t > 0$. Therefore, the design of PML for dispersive waves may be the same as for the non-dispersive case for short time simulation and particularly for short waves. More precisely, at fixed time t this error is affected only by the average absorption rate $\bar{\sigma} = \Sigma(L)/L$, the width of the layer L and the location of the source h while it converges spectrally in the L^∞ norm to 0 when one of these parameters increases.

- Specifically, we do not observe the same behaviour in long time, that is to say, for fixed $T < \infty$ the error behaves for large t as

$$\sqrt{\frac{2T}{t}} + \mathcal{O}\left(\sqrt{\alpha}\right)$$

  and does not necessarily converge uniformly to 0 as t tends to $+\infty$ for all $\bar{\sigma}, L$ and h. This is the main difference (or loss in precision) w.r.t. the non-dispersive case ($\alpha = 0$). However and fortunately, the property of long time stability is conserved since the error remains bounded as t goes to $+\infty$.

- This technique can in particular be used to study the shallow water equations with rotation in order to take into account the effect of the Coriolis force on the behaviour of the absorbing layers.

- Advective Klein-Gordon equation with a parallel mean flow can be analyzed in a very similar way in comparison with the time domain analysis presented for advective acoustics in [16], the same changes of variables can be used as in [21, 5] in order to get rid of the moving referential. However, this sill be not yet obvious at an oblique mean flow.

- The idea of localization proposed in Section 5 is very standard but it opens a wide variety of possibilities in designing absorbing boundary conditions combined with PMLs using other techniques of approximating the square root $\sqrt{s^2 + \alpha^2}$ appearing in $D^{\sigma}_{x_1,\alpha}$.

References

[1] S. Abarbanel and D. Gottlieb. A mathematical analysis of the PML method, J. Comput. Phys. 134 (2) (1997) 357–363.

[2] S. Abarbanel, D. Stanescu, and M. Hussaini. Unsplit Variables Perfectly Matched Layers for the Shallow Water Equations with Coriolis Forces, Computational Geosciences (2003) 7–275.

[3] M. Abramowitz, and I. Stegun. Handbook of Mathematical Functions with Formulas, Graphs, and Mathematical Tables, edited by M. Abramowitz and I. Stegun (Dover, New York, 1964).

[4] Arthur Erdelyi. *Tables of integral transforms.* McGraw-Hill Inc.,US. Vol.1. (1954). Pages 410.

[5] H. Barucq, J. Diaz, and M. Tlemcani. New absorbing layers conditions for short water waves, J. of Comp. Phys., 229 (1) (2010) 58–72.

[6] E. Bécache, S. Fauqueux, and P. Joly, Stability of perfectly matched layers, group velocities and anisotropic waves, J. Comput. Phys. 188 (2) (2003) 399–433.

[7] E. Bécache, P. Joly, and V. Vinoles. On the analysis of perfectly matched layers for a class of dispersive media and application to negative index metamaterials. Math. Comp. 87 (2018), no. 314, 2775–2810.

[8] J.-P. Bérenger. A perfectly matched layer for the absorption of electromagnetic waves, J. Comput. Phys. 114 (1994) 185-200.

[9] J. P. Bérenger. Three-dimensional perfectly matched layer for the absorption of electromagnetic waves, J. of Comp. Phys., 127 (1996) 363–379.

[10] L. Cagniard. Reflection and refraction of progressive seismic waves, McGrawHill, (1962).

[11] F. Collino and P. Monk. The Perfectly Matched Layer in curvilinear coordinates, SIAM J. Scient. Comp. 164 (1998) 157–171.

[12] F. Collino and C. Tsogka. Application of the pml absorbing layer model to the linear elastodynamic problem in anisotropic heteregeneous media, Geophysics 66 (1) (2001) 294–307.

[13] A. T. de Hoop. The surface line source problem, Appl. Sci. Res. B 8 (1959) 349–356.

[14] A. T. de Hoop, P. Van den Berg, and F. Remis. Analytic time-domain performance analysis of absorbing boundary conditions and perfectly matched layers, in: Proc. IEEE Antennas and Propagation Society International Symposium, Vol. 4, (2001), pp. 502–505.

[15] J. Diaz and P. Joly. An Analysis of Higher Order Boundary Conditions for the Wave Equation *SIAM J. Appl. Math.*, 65(5): 1547–1575, 2005.

[16] J. Diaz and P. Joly. A time domain analysis of PML models in acoustics. Comput. Methods Appl. Mech. Engrg. 195 (2006), no. 29-32, 3820–3853.

[17] B. Engquist and A. Majda. Radiation boundary conditions for acoustic and elastic wave calculations, Comm. Pure Appl. Math. 32 (1979) 313-357.

[18] B. Engquist and A. Majda. Absorbing boundary conditions for the numerical simulation of waves, Math. Comp. 31 (1997) 629-651.

[19] S. Fauqueux. Eléments finis mixtes spectraux et couches absorbantes parfaitement adaptées pour la propagation d' ondes élastiques en régime transitoire, Ph.D. thesis, Université Paris IX (2003).

[20] D. Givoli and B. Neta. High-order nonreflecting boundary conditions for the dispersive shallow water equations, Journal of Computational and Applied Mathematics 158 (1) (2003) 49–60.

[21] F. Q. Hu. On absorbing boundary conditions for linearized euler equations by a perfectly matched layer, J. Comp. Phys. (129) (1996) 201–219.

[22] A. YA. Olenko. Upper bound on $\sqrt{x}J_\nu(x)$ and its applications. Integral Transforms and Special Functions Vol. 17, No. 6, June 2006, 455–467.

[23] Andrei D, Polyanin. *Handbook of linear partial differential equations for engineers and scientists*. Boca Raton: Chapman & Hall/CRC, 2002.K.

[24] J. Pedlosky *Geophysical Fluid Dynamics*. Springer, New York, NY, 1987, XIV, pages 710.

[25] K. Watanabe. Cagniard-de Hoop Technique, In: Integral Transform Techniques for Green's Function. Lecture Notes in Applied and Computational Mechanics, Springer, Cham, 76 (2015) 153–204.

[26] L. Zhao and A. C. Cangellaris. A General Approach for the Development of Unsplit Field Time-Domain Implementations of Perfectly Matched Layers for FDTD Grid Truncation, IEEE Microwave and Guided Letters 6 (5) (1996) 209–211.

[27] Lancioni, Giovanni. Numerical comparison of high-order absorbing boundary conditions and perfectly matched layers for a dispersive one-dimensional medium. Comput. Methods Appl. Mech. Engrg. 209/212 (2012), 74–86.